Interactions Between Portland Cement and Carbon Dioxide

F.P. Glasser[1], T. Matschei[1]
[1]University of Aberdeen, Old Aberdeen, AB24 3UE Scotland, UK

Abstract

The carbonation process of a model cement has been calculated. Mineralogical and volume changes are shown as functions of the degree of carbonation, defined as mass of CO_2/mass of cement. Thirteen zones are predicted to occur. The features of normal carbonation are (i) carbonation of portlandite before C-S-H, (ii) formation of ettringite-thaumasite solid solution preceding thaumasite and (iii) development of strätlingite.

1. Introduction

Carbonation, resulting in reaction between gaseous and dissolved CO_2 species and the constituent solids of cement pastes, occurs in a wide variety of exposures. The atmosphere contains about 380 ppm CO_2 gas, equivalent to a pressure of 3.55e-4 bars. If carbonation goes to completion at the relatively high CO_2 partial pressure of air, all constituent phases of Portland cement will react giving mixtures of calcium carbonate and other appropriate solids. But reaction can occur over a wide range of CO_2 pressures as shown in Table 1.

Table 1: Range of CO_2 pressures relevant to cement systems

control	P_{CO_2} approximate 25° C numerical value (bars)
$CaCO_3$ (solid) with $Ca(OH)_2$ to buffer pH)	7.39 e-14
Atmosphere (standard)	3.55 e-4
Atmosphere (accelerated)	1.0 maximum (without pressurisation)
Supercritical CO_2	50

The extent of reaction depends on the activity of CO_2 (including its dissolved species, CO_2, HCO_3^- and CO_3^{2-}) as well as the total mass available at that pressure. We will concentrate on the low pressure range, < 1 bar at saturated relative humidity. One belief is that $CaCO_3$ is inert in Portland cement paste, but we have shown it is reactive up to a critical saturation value, depending on cement composition [1]. Some may doubt that low CO_2 pressures, such as those sustained by $CaCO_3$, have physical significance. Despite the low partial CO_2 pressures achieved in cement systems a large total mass of CO_2 may be present in solids, e.g., as calcite, albeit in relatively insoluble form; This large mass of carbonate implies that if potential for reaction exists it will occur. This potential has been quantified using thermodynamics in conjunction with a suitable database and experimentally verified [1].

2. Experimental.

Calculations (which we regard as an experimental tool) have been made using GEMS [2], a software to minimise the free energy of a given system. An advantage of calculation is flexibility in terms of being able to change input parameters. GEMS also computes mass balances, giving the composition of the aqueous phase as well as tabulating coexisting solids. The database enabling thermodynamic calculations is partly given in [2] supplemented by [4]. Additional data for thaumasite were estimated from [5]. C-S-H was treated as a solid solution [6] but the lower limit of Ca/Si was restricted to 0.83 (see [7]). The following calculations display applications of the database to explore the carbonation process. All calculations relate to 25°C and 1 bar total pressure. The calculations automatically speciate CO_2 according to concentration, pH and temperature. The software simulates equilibrium and does not immediately cope with situations in which composition gradients occur, as in atmospheric carbonation. Therefore we initially concentrate on defining the internal equilibrium and, from knowledge of these states, undertake a kinetic analysis of dynamic carbonation.

3. Atmospheric carbonation

3.1. Basis of calculation

The present computations use a simplified model cement composition consisting of initially 68.5 wt.-% CaO, 22 wt.-% SiO_2, 4.5 wt.-% Al_2O_3 and 5 wt.-% $CaSO_4$ (~2.9 wt.-% SO_3): 100 g of this cement are reacted with 50 g water (w/c = 0.5). Alkalis and iron oxides are omitted to reduce the complexity of the system. The mineralogical consequences of the dynamic interaction of hydrated cement paste with atmospheric CO_2 were investigated by adding increasing amounts of CO_2 to the model cement.
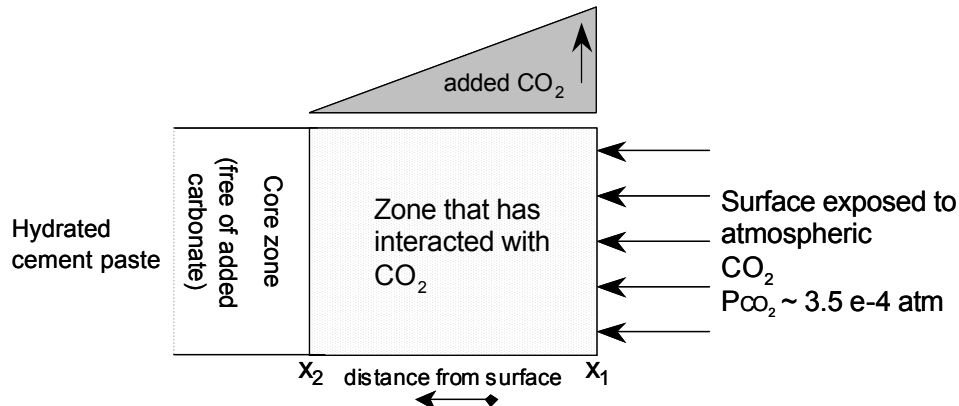

Fig. 1: Schematic, showing CO_2 added from the atmosphere. (Schematic CO_2 profile (top) and carbonated zone (bottom) are shown without detail.)

The calculations conserve mass except for gain of CO_2. The amount of CO_2 added to the hydrated model mixture is increased until we reach atmospheric conditions and the outer zone equilibrates with an unlimited amount of standard atmosphere (P_{CO_2} ~3.5 e-4 atm). The course of reaction is conditioned by (i) high carbonate activities in the atmospheric reservoir and (ii) a CO_2 concentration gradient developing spontaneously within the paste as shown schematically in Fig. 1 and (iii) the assumption that local equilibrium is attained at each point along the CO_2 gradient

3.2. Mineralogical changes due to carbonation

Fig. 2 shows the mineralogical changes arising in the course of carbonation of the hydrated model cement along the x-axis of Fig.1 between depths X_2 and X_1, the latter being a fully carbonated outer layer in equilibrium with atmospheric CO_2 (P_{CO_2} ~ 3.5 e-4 atm).
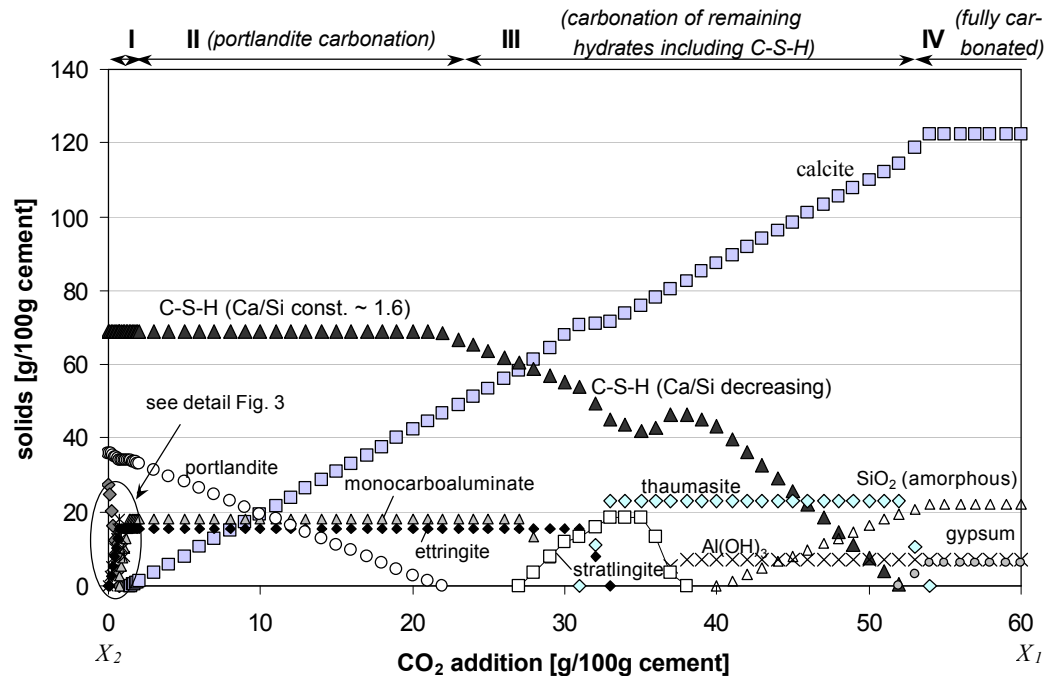

Fig. 2: Impact of carbonation on mass-balance of hydrated model cement paste at 25°C at saturated relative humidity. Note that the calculated phase distribution is a function of CO_2 addition; thus the diagram represents the sequence of different zones, not their relative physical thicknesses.

Fig. 2 demonstrates that the sequence of mineralogical change during carbonation is a complex process involving the mass of CO_2 that has reacted with cement hydrates as well as the partial pressure of CO_2 at the selected point. Calcite does not develop immediately but once it becomes stable, the amount of calcite increases progressively with increasing amounts of CO_2 added. However a complex mineralogical zonation develops. Transformations from one zone to another require addition or

removal of CO_2 at constant pressure, thus creating a series of internal carbonate buffers for P_{CO_2}. Many stages also involve loss of water, not shown in Fig. 2 but described subsequently.

To systemise reactions with CO_2, we start with the earliest stages of carbonation, when CO_2 is first available. Point X_2 represents the persistent phase assemblage of a carbonate-free Portland cement (Zone 0, table 2). The paste consists mainly of C-S-H, portlandite and a monosulfoaluminate-type AFm-phase. Previous studies have shown that the AFm phase plays a key role with respect to the interactions with carbonate at low P_{CO_2}. Fig. 3 shows enlarged detail of Fig.2, applicable to these conditions (CO_2 < ~1% of the cement). In Zone I *a)* monosulfo-aluminate depletes rapidly and hemicarboaluminate is formed as P_{CO_2} increases. The released sulfate reacts with a part of the aluminate and portlandite to form ettringite, AFt. With further increases of CO_2, hemicarboaluminate decomposes to monocarboaluminate in Zone I *b)*. Note that although significant uptake of CO_2 is occurring, calcite is not formed. However presently-available Portland cements may contain significant amounts of limestone and/or other carbonate sources that conclude stage I reactions prior to atmospheric carbonation [1].

Table 2: Calculated phase assemblages in the course of carbonation at 25°C

Zone		Solid phase assemblage[1]
0 *(intact core zone)*		C-S-H (Ca/Si ~ 1.65), portlandite, monosulfoaluminate (ss)
I *(early stages)*	*a)*	C-S-H (Ca/Si ~ 1.65), portlandite, monosulf.$\downarrow$, hemicarb.$\uparrow$, ettringite$\uparrow$
	b)	C-S-H (Ca/Si ~ 1.65), portlandite, hemicarb.$\downarrow$, monocarb.$\uparrow$, ettringite
II *(portlandite carbonation)*		C-S-H (Ca/Si ~ 1.65), portlandite$\downarrow$, monocarboaluminate, ettringite, calcite$\uparrow$,
III *(transition zone; carbonation of remaining hydrates)*	*a)*	C-S-H (Ca/Si ~ 1.65 $\rightarrow$ 1.4)$\downarrow$, monocarboaluminate, ettringite, calcite$\uparrow$
	b)	C-S-H (Ca/Si ~ 1.4 $\rightarrow$ 1.3)$\downarrow$, monocarb.$\downarrow$, ettringite, strätlingite$\uparrow$, calcite$\uparrow$,
	c)	C-S-H (Ca/Si ~ 1.3)$\downarrow$, ettringite$\downarrow$, calcite$\uparrow$, strätlingite $\uparrow$, thaumasite$\uparrow$
	d)	C-S-H (Ca/Si ~ 1.3 $\rightarrow$ 1.1)$\downarrow$, calcite$\uparrow$, strätlingite, thaumasite
	e)	C-S-H (Ca/Si ~ 1.1 $\rightarrow$ 1.0)$\uparrow$, calcite$\uparrow$, strätlingite $\downarrow$, thaumasite, Al(OH)$_3\uparrow$
	f)	C-S-H (Ca/Si ~1.0 $\rightarrow$ 0.83) $\downarrow$, calcite$\uparrow$, thaumasite, Al(OH)$_3$,
	g	C-S-H (Ca/Si ~ 0.83) $\downarrow$, calcite$\uparrow$, thaumasite, Al(OH)$_3$, SiO$_2$(amorphous) $\uparrow$
	h)	SiO$_2$(amorphous), calcite$\uparrow$, thaumasite$\downarrow$, Al(OH)$_3$, gypsum$\uparrow$
IV *(fully carbonated)*		SiO$_2$(amorphous), calcite, Al(OH)$_3$, gypsum

[1] additionally aqueous phase present in all assemblages; $\uparrow$ increasing and $\downarrow$ decreasing amounts
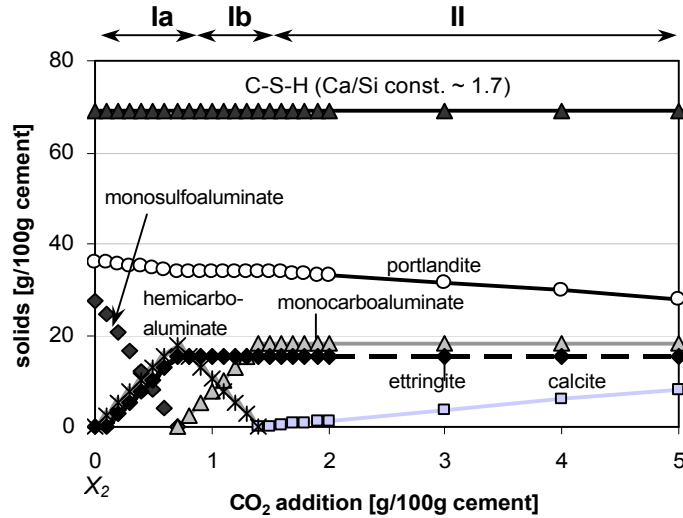
Fig. 3: Impact of carbonation on mass-balance of hydrated model cement paste (enlarged detail from Fig. 2). Zones (top) are defined in Table 2.

The development of carbonate-containing phases in real cements is further complicated by the presence of sulfate which (i) competes with carbonate for available Al by forming ettringite (AFt) as well as (ii) competing for anion sites in AFm, by forming sulfate AFm and (hydroxy-sulfate)- AFm solid solutions. Previous studies have delineated the broad outlines of the stability relations in systems with both sulfate and carbonate [1][2][8,9][8] as well as the impact of alkalis on the equilibria [10,11]. Development of sulfate distribution models is presented elsewhere in this Congress [12] where it is shown that sulfate buffering reactions, parallel to those for carbonate, develop spontaneously in cement systems.

Fig. 2 shows that with increasing amounts of CO_2 the amount of port-landite diminishes rapidly and calcite forms (Zone II). Beside changes in the AFm chemistry in the early stages of carbonation, portlandite is pre-ferentially carbonated while C-S-H remains unaffected. Thus calcite, monocarboaluminate, portlandite and C-S-H comprise the assemblage defining Zone II (Table 2).

However once portlandite is fully carbonated the remaining hydrates increasingly react with carbon dioxide to form calcite, amongst other phases. Thus Zone III (Fig. 2) can be designated as a *transition zone* between the high pH, portlandite-buffered system to a fully carbonated matrix. In Zone III, a significant decrease in pore fluid pH will occur, from > 12 to 10 or less. However as C-S-H is progressively carbonated and its silica content increases, decomposition of ettringite commences. Fig. 2 shows that as ettringite decomposes, thaumasite forms. We presently lack a thermodynamic model to describe ettringite-thaumasite solid solutions

so the computer is instructed to generate both ettringite and thaumasite; it is probable that the correct interpretation is that ettringite composition shifts, with formation of an ettringite-thaumasite solid solution, as a precursor to thaumasite formation [5]. Additionally strätlingite (C_2ASH_8) is predicted to develop from alumina released by the decomposition of monocarboaluminate and silica from C-S-H. The supplementary construction, Fig. 4, shows how the Ca/Si ratios of C-S-H remain unaffected (~1.65) as long as portlandite saturation is maintained (Zones I and II). But once portlandite is depleted, the Ca/Si ratio of C-S-H decreases progressively in Zone III from ~1.65 to ~0.8, the lower limit of Ca/Si-ratios, before free amorphous hydrated silica forms. The carbonation of strätlingite to a mixture of $Al(OH)_3$ and C-S-H explains the shoulder in the C-S-H curve at ~ 35 - 40 g CO_2/100g cement.
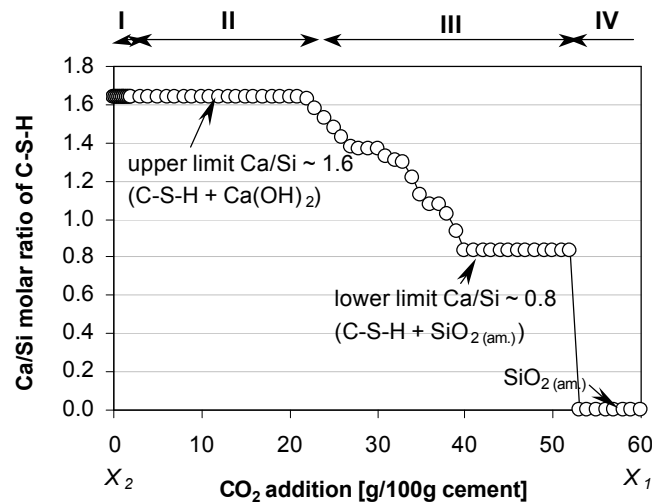

Fig. 4: Development of Ca/Si ratio of C-S-H with increasing additions of CO_2 to hydrated model cement

Thaumasite is computed to be very persistent and stable at higher CO_2 activities. However, in agreement with [13,14], its formation and persistence in the fully carbonated zone is not possible. As shown in Fig. 2, thaumasite may form in a layer close to the fully carbonated zone but thaumasite itself is not stable if exposed to environments conditioned by atmospheric CO_2 (P_{CO_2}~ 3.5 e-4 atm). Formation of thaumasite is only possible if sufficient water is available i.e. at high relative humidity but ettringite, resorbed in the course of thaumasite formation, may provide necessary water.

Finally Zone IV (Fig. 2) represents the fully carbonated outer layer, which is calculated to be in equilibrium with air with a CO_2 partial pressure of ~ 3.5 e-4 atm (as occurs in an open system with an unlimited supply of air). In agreement with numerous investigations calcite, gypsum, $Al(OH)_3$ and amorphous silica are the stable phase assemblage.

Many of the phase assemblages of Table 2 have been observed experimentally. Kuzel [15] has shown that in a virtually carbonate-free OPC with a SO_3/Al_2O_3-ratio < 1, C-S-H, portlandite and monosulfoaluminate (solid solution) will form at 25°C. In agreement with thermodynamic calculations by Matschei et al. [1][3] and Damidot et al. [11] and experimental results by Kuzel et al. [8] hemicarbonate will form at low carbonate activities but hemicarbonate will decompose to monocarbonate with increasing carbonate activities and is not stable under calcite-saturated conditions. Due to the decomposition of monosulfoaluminate, sulfate is released resulting in formation of ettringite [1][3][8,9]. As shown by Locher [16] and in agreement with thermodynamic calculations by Damidot and Glasser [17], strätlingite is not stable in contact with portlandite and is predicted to coexist with C-S-H having low Ca/Si-ratios, $\leq$ 1.4. The formation of thaumasite in the course of carbonation may be surprising, however as shown by Blanco-Varela et al. [18], thaumasite formed in carbonated mortars, without additional carbonate and sulfate sources, after 5 years storage in water at 5°C. Furthermore, and in agreement with calculations, Diamond [19] showed the formation of thaumasite in carbonated mortars in California at temperatures > 15°C. Calculations by Damidot et al. [20] show that thaumasite is predicted to be stable at pH $\geq$ 8.5 at 25°C, corresponding to phase assemblage III *h),* Table 2. Bellmann [14] records the persistence of the phase assemblage of thaumasite, SiO_2 (amorphous) and calcite for more than 7 months at pH ~ 8.2 at 8°C.
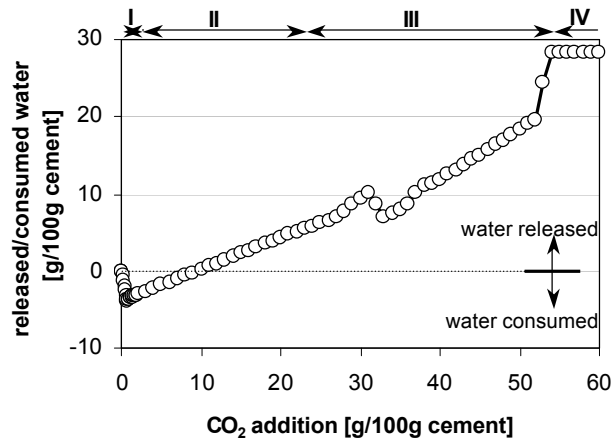

Fig. 5: Water release and consumption due to carbonation of hydrated model cement paste

It is well known that carbonation of cement paste results in a release of water because the main carbonation product, calcite, is anhydrous. Fig. 5, in conjunction with Fig. 2, shows the water balances in the course of carbonation; the overall pattern is of water release, but water is also *consumed* at two stages: one in the early stages of carbonation as ettringite forms and again at ~30g CO_2 as the amount of thaumasite increases.

3.3. Volume changes due to carbonation

All practical observations on cement systems undergoing carbonation suggest that shrinkage -termed "carbonation shrinkage" - is a real phenomenon. Yet the gain of CO_2 and related mineralogical changes lead to a calculated increase of the total volume (including the aqueous phase) (Fig. 6). Water release is mainly responsible for the volume increase of the carbonated cement paste but is not necessarily retained, so we consider mainly the volume changes of the solids. The reaction of portlandite forming calcite in Zone II leads to a slight increase in volume, resulting mainly in a densification of the matrix. However the total solid volume increase (~ 3.2 vol-%) is small compared to other potential carbonation reactions occurring in Zones I and III (compare Figs. 6 - 8).

Fig. 7 shows the total volume changes at low additions of CO_2 at early stages of carbonation; see also [1] for explanation. Thus the solids volume will be affected significantly during early-stage carbonation. In the model cement, a volume increase of ~ 6 vol-% will be observed due to the conversion of monosulfoaluminate to ettringite and hemicarboaluminate (see Fig. 8). However the % volume increase is sensitive to the cement SO_3/Al_2O_3 ratio [1]. Commercial cements are likely to contain sufficient amounts of carbonate to reduce or eliminate the impact of these early-stage reactions. But a volume increase is also calculated to occur in Zone III (Figs. 6 and 8) where thaumasite or ettringite-thaumasite solid solutions are predicted to form.
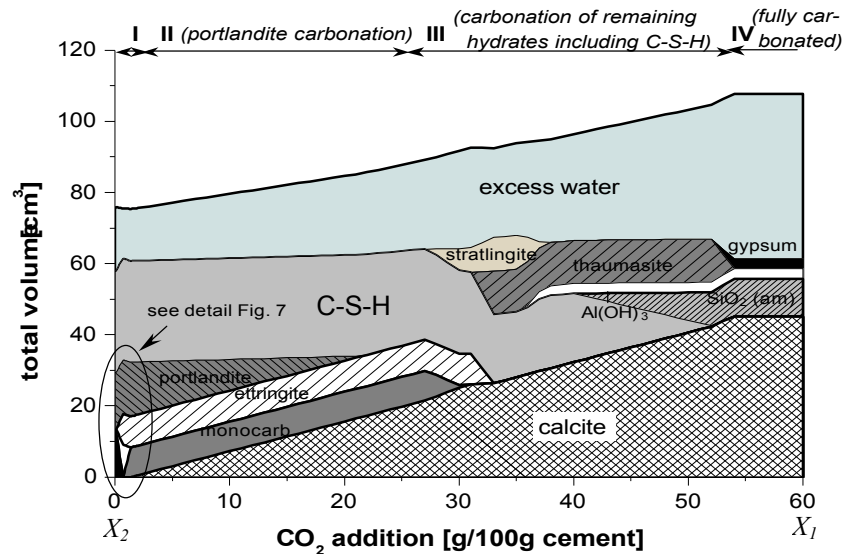

Fig. 6: Volume changes due to carbonation of hydrated model cement paste at 25°C at saturated relative humidity. Note that the calculated phase distribution is a function of CO_2 addition; thus the diagram represents the sequence of different zones, not their relative physical thicknesses. The "excess water" is the sum of unconsumed mix water (pore solution) and net water liberated by carbonation. Depending on relative humidity at the cement-air interface some or all of this water may be lost by evaporation.
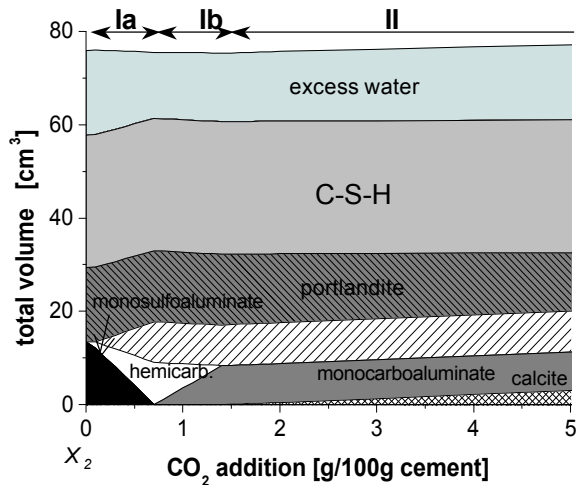
Fig. 7: Volume changes in early stages of carbonation (detail from Fig. 6)
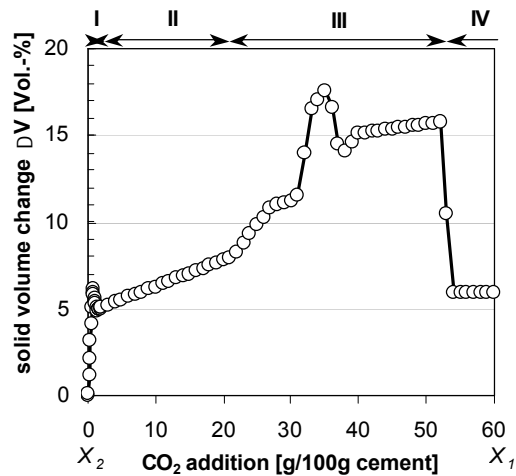
Fig. 8: Solid percentage volume increase due to carbonation of hydrated model cement paste

Due to the simultaneous formation of thaumasite and strätlingite, as well as related previous carbonation reactions in Zone I and II, a maximum total solid increase of ~ 18 vol-% is calculated (Fig. 8). This implies significant recrystallisation in Zone III so as to fill pore spaces. Thus while a dense layer is predicted to develop directly behind the fully carbonated zone the permeability with respect to CO_2 migration into the matrix may be significantly slowed by filling of pores. The pore filling effect may also account for the slight increases of strength attending carbonation.

3.4. Changes of the aqueous phase composition

Fig. 9 shows the related changes of the aqueous phase arising in the course of carbonation.
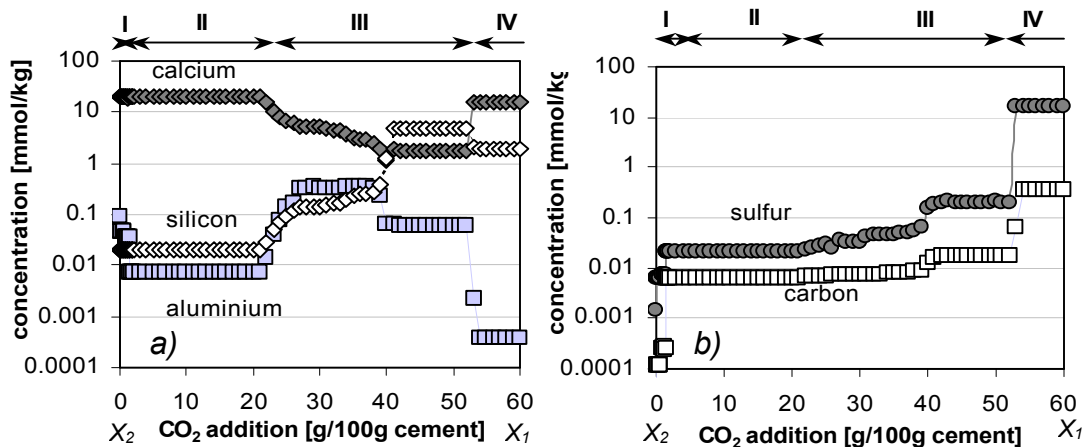

Fig. 9: Changes of the aqueous phase composition due to carbonation of hydrated model cement at 25°C (all species included in total dissolved molalities of components)

Fig. 9a shows that calcium and silicon concentrations remain nearly constant in Zone I and II, but changes of the phase constitution of the aluminium- and sulfur-bearing phases affect both aluminium and sulfur concentrations in Zone I (Fig 9b). Whereas the concentration of aluminium decreases by one order of magnitude, dissolved sulfur and carbon (total concentration of all species) increase significantly in the course of increasing carbonation. No significant changes in ion concentrations occur in Zone II: the aqueous phase pH is buffered by the assemblage C-S-H (Ca/Si~1.65) portlandite, calcite, monocarboaluminate and ettringite. However once portlandite is depleted significant changes occur in Zone III. With decreasing Ca/Si-ratios of the C-S-H, calcium concentrations decrease from ~ 20 mmol/kg to ~ 1 mmol/kg, whereas silicon concentrations increase until a steady state is reached towards the end of Zone III. Aqueous aluminium concentrations increase by more than one order of magnitude compared to Zone II as monocarboaluminate and ettringite decompose: thus total sulfur and carbon concentrations increase almost reaching the equilibrium concentrations (total sulfur ~ 15.9 mmol/kg, total dissolved carbon (mainly as HCO_3^-) is ~ 0.36 mmol/kg) in the fully carbonated Zone IV. At atmospheric CO_2 partial pressure the aqueous phase (composition, pH) is conditioned by the assemblage gypsum, calcite, $Al(OH)_3$ and amorphous SiO_2. Calcium concentrations increase significantly whereas the aluminium solubilities decrease by ~ 2 orders of magnitude mainly due to its low solubility at pH ~ 7 (Fig. 10). Silicon concentrations decrease only slightly in the fully carbonated Zone IV.
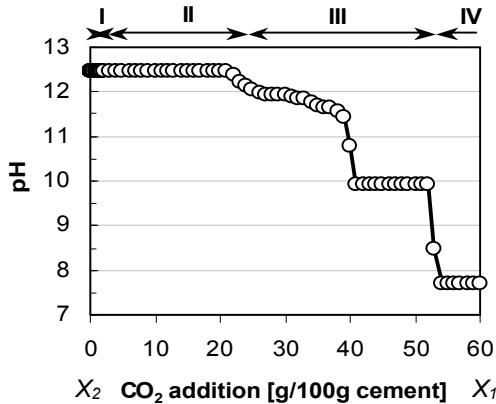

Fig. 10: pH of aqueous phase in the course of carbonation of the hydrated model cement paste
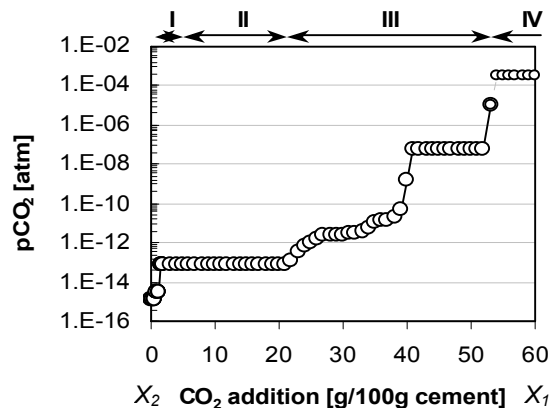
Fig. 11: CO$_2$ partial pressure in the course of carbonation of the hydrated model cement paste

The pH buffering by cement solids passivates embedded steel. Fig. 10 shows the evolution of pH with increasing CO_2. As long as portlandite is present the pH is buffered at ~12.5 at 25°C in Zones I and II: note that alkalies are not considered in the present approach. Once portlandite is depleted, the pH is mainly buffered by C-S-H. However with decreasing

Ca/Si ratio of the C-S-H, the pH decreases in Zone III from ~12.5 to ~9.9 at Ca/Si ~ 0.8. Thus only small amounts of C-S-H with low Ca/Si ratios, ~0.8, are theoretically sufficient to buffer the pH of the solution to ~ 10. In practice carbonation depth is tested with a phenolphtalein/alcohol mixture and the "noncarbonated" zone is indicated by a red colouration having pH-values between 8.2-10. It is interesting to note this would indicate only the fully carbonated layer, and thus significant earlier carbonation reactions occurring in Zones I-III of the structure fail to be detected by this method.

Fig. 11 demonstrates the change of the corresponding CO_2 partial pressure with respect to increasing CO_2 additions to the hydrated model cement paste. In Zone I, where calcite is absent, the resulting P_{CO_2} is very low (~1 e-15 atm). The CO_2 partial pressure increases to ~ 7 e-14 atm in Zone II where calcite first appears with monocarboaluminate. In Zone III, where calcite and thaumasite are the main carbonate phases, P_{CO_2} increases until it reaches atmospheric ~ 3.5 e-4 atm. A comparison with the mineralogical mass balances (Fig. 2) shows that thaumasite is a very persistent phase with respect to carbonation and is stable over a wide range of CO_2 pressures. Our calculations, predicting thaumasite to be stable in the range ~1e-12 atm $\leq P_{CO_2} \leq$ ~1e-5 atm, are in good agreement with Bellmann [14] who calculated a similar upper limit of P_{CO_2}. The gradual increase in thaumasite stability with rising P_{CO_2}, resulting first in formation of ettringite-based solid solutions [18] and subsequently in thaumasite, gives credence to the widespread belief that ettringite is an essential precursor to thaumasite [20,21]. The phase data do not require this be so, but in situations where thaumasite forms as a result of rising P_{CO_2}, this is predicted to be the normal progression at saturated relative humidity.

4. Discussion

The dimensional changes associated with carbonation have long been a subject of interest. Lea [23] summarises decades of experience showing that slight shrinkage of cement paste and concrete normally occurs upon carbonation although the amount of shrinkage is difficult to deconvolute from other changes that affect dimensional stability, for example wet- dry cycling. However Lea also notes that carbonation of portlandite is expansive and gives a value of 11% expansion. Of course portlandite is only one component of a hardened Portland cement paste so this value is not necessarily directly applicable to cement pastes. In recent decades we have also been reminded of the many mechanisms for stress relief in a Portland cement undergoing reaction. The paste contains considerable porosity and provided crystallisation of product phases occurs in pores, no physical expansion need occur even if the volume of solid products exceeds that of reactants. Moreover, the microstructure is not necessarily immutable: phase changes can reconstitute the microstructure.

However in the present case, overall liberation of water also occurs. Fig. 6 shows that if this water is retained, a large potential for expansion exists. But it is unlikely that water is retained except in the short term: carbonation can only be sustained if gaseous and dissolved CO_2 continues to diffuse inwards and, if diffusion paths exist for CO_2, it is likely that water in excess of that required to equilibrate with the local humidity can also diffuse out. It is likely therefore that water liberated by carbonation is ephemeral but in the course of its transient formation and persistence, is available to facilitate recrystallisation. In principle the water "front" associated with advancing carbonation could be imaged directly by high resolution NMR and techniques for such studies are being developed. Attention is also directed to the conclusion of the title study that in a CO_2 gradient, portlandite is carbonated preferentially to C-S-H. In cement matrices containing physically large portlandite crystals there is potential for local stress accumulation by this mechanisms. Again, it remains to be determined if this mechanism actually operates and if so, what regimes are favourable for its operation.

If we look at the bulk volume changes including all solids, an expansive trend, albeit slight, is evident. This probably underlies the conclusions that carbonation improves strength slightly: as carbonation progresses without expansion total porosity decreases while the changing distribution of pores in the course of recrystallisation also contributes to the observed shrinkage. There is however need for further research to link the dimensional stability of cements, mortars and concretes under-going carbonation with the mineralogical and mass balance changes.

The pH gradients conditioned by progressive carbonation are shown to be complex. Not surprisingly the position of the carbonation "front", as revealed by phenolphthalein, is simplistic. Nevertheless it is a good indicator of the boundary between regions of low and high corrosion potential with respect to protection for embedded steel. Provided it is used as such, and no more, it is a satisfactory and rapid test suitable for use in the field. But is should not be used to deduce reaction kinetics of what is, after all, a complex process.

5. Acknowledgement

6. References

[1] Matschei, T.; Lothenbach B.; Glasser, F.P.: The role of calcium carbonate in cement hydration. *Cement and Concrete Research*, in press 2007

[2] Kulik, D.; Berner, U.; Curti, E.: Modelling chemical equilibrium partitioning with the GEMS-PSI code. *PSI Scientific Report* 2003, Vol. IV, 109-122,

[3] Matschei, T.; Lothenbach B.; Glasser, F.P.: The AFm-phase in Portland cement. *Cement and Concrete Research*, 2007, **37**, 118-131

[4] Matschei, T.; Lothenbach B.; Glasser, F.P.: *in preparation*

[5] Macphee, D.; Barnett, S.: Solution properties of solids in the ettringite—thaumasite solid solution series. *Cement and Concrete Research,* 2004, **34**, 1591-1598

[6] D.A. Kulik, M. Kersten, Aqueous solubility diagrams for cementitious waste stabilization systems: II, End-member stoichiometries of ideal calcium silicates hydrate solid solutions, Journal of the American Ceramic Society, 2001, **84**, 3017-3026.

[7] Taylor, H.F.W.: *Cement Chemistry* (2nd Edition), Thomas Telford Publishing, London, 1997

[8] Kuzel, H.J.; Poellmann, H: Hydration of C_3A in the presence of $Ca(OH)_2$, $CaSO_4 \cdot 2H_2O$ and $CaCO_3$. *Cement and Concrete Research*, 1991, **21**, 885-895

[9] Herfort, D.: Relationship between Strength, Porosity and Cement Composition.: unpublished paper, Nanocem workshop on the "Relation between Microstructure and Mechanical Properties" Czech Technical University, Prague, 2004

[10] Damidot, D.; Glasser, F.P.: Thermodynamic investigation of the CaO-Al_2O_3-$CaSO_4$-H_2O-System at 25 °C and the influence of Na_2O. *Cement and Concrete Research*, 1993, **23**, 221-238

[11] Damidot, D.; Stronach, S.; Kindness, A.; Atkins, M.; Glasser, F.P.: Thermodynamic investigation of the CaO-Al_2O_3-$CaCO_3$-H_2O closed system at 25 °C and the influence of Na_2O. *Cement and Concrete Research,* 1994, 24, 563-572

[12] Matschei, T., Skapa, R.; Lothenbach, B.; Glasser, F.P.: The distribution of sulfate in hydrated Portland cement paste. Submitted to *Proceedings of the 12th Intern. Congress on the Chemistry of Cements,* Montreal, 2007

[13] Collet, G.; Crammond, N.J., Swamy, R.N.; Sharp, J.H.: The role of carbon dioxide in the formation of thaumasite

[14] Bellmann, F.: On the formation of thaumasite $CaSiO_3 \cdot CaSO_4 \cdot CaCO_3 \cdot 15H_2O$: Part II.: *Advances in Cement Research,* 2004, **16**, 89-94

[15] Kuzel, H.J.: Initial hydration reactions and mechanisms of delayed ettringite formation in Portland cement. Cement and Concrete Research, 1996, 26, 195-203

[16] Locher, F.W.: Hydraulische Eigenschaften von kalkreichen Glaesern des Systems $CaO-Al_2O_3-SiO_2$. Schriftenreihe der Zementindustrie, Heft 25, Forschungsinstitut der Zementindustrie, Duesseldorf, 1960

[17] Damidot, D.; Glasser, F.P.: Investigation of the $CaO-Al_2O_3-SiO_2-H_2O$-System at 25 °C by thermodynamic calculations. *Cement and Concrete Research*, 1995, **25**, 22-28

[18] Blanco-Varela, M.T.; Aguilera, J.; Martinez-Ramirez, S.: Effect of cement C3A content, temperature and storage medium on thaumasite formation in carbonated mortars. *Cement and Concrete Research*, 2006, **36**, 707-715

[19] Diamond, S.: Thaumasite in Orange County, Southern California: an inquiry into the effect of low temperature. *Cement and Concrete Composites,* 2003, **25**, 1161-1164

[20] Damidot, D.; Barnett, S; Glasser, F.P.; Macphee, D.: Investigation of the $CaO-Al_2O_3-SiO_2-CaSO_4-CaCO_3-H_2O$ system at 25°C by thermodynamic calculation. *Advances in Cement Research,* 2004, **16**, 69-76

[21] Crammond, N.J.: The thaumasite form of sulfate attack in the UK. *Cement and Concrete Composites,* 2003, **25**, 809-818

[22] Koehler, S.; Heinz, D.; Urbonas, L.: Effect of ettringite on thaumasite formation. *Cement and Concrete Research,* 2006, **36**, 697-706

[23] Lea, F.M.: The Chemistry of Cement and Concrete. 3rd Edition, Edward Arnold Publishers Ltd, 1970